Design and fabrication of zero-group-velocity Lamb wave resonator onto silicon nitride/ aluminum nitride suspended membrane

Cite as: AIP Conference Proceedings **1990**, 020013 (2018); https://doi.org/10.1063/1.5047767
Published Online: 23 July 2018

Cinzia Caliendo, Ennio Giovine and Muhammad Hamidullah

Design and Fabrication of Zero-Group-Velocity Lamb Wave Resonator onto Silicon Nitride/Aluminum Nitride Suspended Membrane

Cinzia Caliendo[1,a)], Ennio Giovine[1,b)], Muhammad Hamidullah[1,c)]

[1] *Institute for Photonics and Nanotechnology, (CNR-IFN), via Cineto Romano 42, 00156 Rome, Italy*

[a)] Corresponding author: cinzia.caliendo@cnr.it
[b)] ennio.giovine@ifn.cnr.it
[c)] hamidullah@ifn.cnr.it

Abstract. The propagation of the Lamb-like modes along an AlN/Si_3N_4 thin suspended membrane was simulated in order to exploit the zero group velocity (ZGV) resonant conditions, i.e. the frequencies where the mode group velocity vanishes while the phase velocity remains finite. A ZGV micro electroacoustic resonator employing only one interdigital transducer (IDT) and no reflectors was designed that is based on the propagation of the first quasi symmetric mode qS_1 at frequency of about 1.63 GHz. The device was fabricated directly onto commercially available thin suspended Si_3N_4 membrane, 200 nm thick, in square silicon supporting frame (200 μm thick). The Cr/Au interdigital transducer (IDT), with periodicity of 10 μm, was fabricated by electron beam lithography (EBL) directly onto the Si_3N_4 membrane; then the piezoelectric AlN layer was grown onto the membrane at room temperature by rf reactive magnetron sputtering technique. The technological feasibility of the ZGV resonator on commercial Si_3N_4 suspended membrane is demonstrated and preliminary experimental results are shown.

INTRODUCTION

Lamb waves are acoustic modes that propagate along finite thickness plates with traction-free surfaces. These waves propagate in two types of modes, the symmetrical (S) and the anti-symmetrical (A) modes: in the S modes, the plate displacements are symmetrical with respect to the mid plane of the plate, while in the A modes it is anti-symmetrical. There are infinite number of modes (S_n and A_n) existing in a plate, and n is the modes order. The modes are dispersive as their phase and group velocity depend on the plate thickness-to-wavelength ratio. In case of bi-layered composite plates, the waveguide symmetry with respect to the mid plane of the plate is lost and the modes can no more be identified as symmetric or antisymmetric: the modes are generically distinguished by a number in the order in which they appear along the frequency axis. For specific modes and plate thickness values the group velocity v_{gr} can even reach negative values. For some branches of the phase velocity dispersion curves, a strong resonance can be found that occurs at the frequency minimum: at this frequency, a zero-group velocity (ZGV) Lamb mode occurs that is characterized by a vanishing group velocity combined with a non-zero wave number: this phenomenon appears in both monolayer (isotropic and anisotropic) as well as in multilayer plates. As a result, a stationary non-propagating mode is obtained that corresponds to a local resonance in the response spectrum of the plate where the Lamb modes travel.

The propagation of Lamb modes along piezoelectric plates is excited and detected by metal interdigital transducer (IDTs) as for the surface acoustic waves (SAWs). In the SAW resonators (SAWRs) the acoustic energy is confined to a depth of roughly one wavelength from the surface, inside the planar resonant cavity that consists in one IDT and two grating reflectors positioned at both sides of the IDT [1]. The most severe limitation of the SAWRs are the low velocity that limits the resonant frequency to about 2.0 GHz and the low Q factor when using standard

NANOINNOVATION 2017
AIP Conf. Proc. 1990, 020013-1–020013-7; https://doi.org/10.1063/1.5047767
Published by AIP Publishing. 978-0-7354-1706-9/$30.00

microelectronic manufacturing techniques. Lamb Wave Resonators (LWRs) are based on two different configurations. One is a grating-type configuration employing metal reflective gratings, similar to the one-port SAWRs: the Lamb mode energy, distributed throughout the bulk of the crystal, travels along the surface and, as in a SAWR, is reflected by the gratings to reduce the energy loss [2]. Another example of LWR includes only the IDT and no reflectors: the Lamb wave modes propagate in the piezoelectric thin membranes suspended by tethers until they reflect from the suspended *free edges* of the thin plate [3]. These LWRs enable a higher Q and higher resonant frequencies than the SAWRs. Another resonator based on the Lamb modes propagation is the ZGVR: it requires only one IDT and no reflectors. For specific plate thickness-to-wavelength ratio values, a strong resonance occurs that is characterized by a vanishing group velocity combined with a non-zero wave number: at this ZGV point the acoustic energy cannot be carried away from the IDT, leading to a stationary non-propagating mode. The ZGVRs are capable of solving the low frequency and Q limitation faced by the SAWRs. Moreover the ZGVRs require a technology simpler than that required by the free edges resonators and have dimensions smaller than those of the LWRs or SAWRs due to the absence of the reflectors, thus allowing an increase in the number of devices that can be hosted onto a single chip.
We studied the acoustic field profile of the Lamb modes travelling across thin AlN/Si_3N_4 plates and found two ZGV points at two specific plate thickness-to-wavelength ratio values, corresponding to the first quasi-symmetric mode qS_1 and the second quasi-antisymmetric mode qA_2.

To the authors' best knowledge, only a few studies consider the topic of ZGV micro-acoustic resonators on thin suspended acoustic waveguides: references [4, 5] describe the design, fabrication and test of the ZGVR based on the qS_1 mode travelling along an AlN membrane. The device employs a (0002)-oriented AlN thin suspended membrane, 2.5 μm thick, and a λ/8 split-electrode IDT (with wavelengths λ of about 8.0 - 8.8 μm) patterned on top of the piezoelectric layer: the device was acoustically isolated by etching the Si substrate from the backside.

In the present paper, as opposed to the AlN-based ZGVRs described in references 4 and 5, we describe the fabrication of a c-AlN/Si_3N_4-based ZGVR by using a different technological approach that consists in the fabrication of the Cr/Au IDT by electron beam lithography (EBL) directly onto the Si_3N_4 membrane, 200 nm thick; then the piezoelectric AlN layer (2.8 μm thick) was grown onto the membrane at room temperature by rf reactive magnetron sputtering technique. The X ray diffraction measurement revealed the (0002) preferential orientation of the AlN deposited onto the Si_3N_4 suspended membrane: the full width at half maximum FWHM of the rocking curve was about 2°. Then the ZGVR scattering parameter S_{11} was measured by a vectorial network analyser connected to a rf probe station: the 1.63 GHz resonance corresponding to the theoretically expected first quasi-symmetric mode ($q\text{-}S_1$) ZGV mode was observed. The feasibility of the ZGVR on commercial Si_3N_4 suspended membrane is demonstrated and preliminary results concerning the $q\text{-}S_1$ based ZGVR are presented.

SIMULATION STUDY OF LAMB MODES IN ALN/SI$_3$N$_4$ MEMBRANES

The propagation of Lamb waves along a AlN/Si_3N_4 thin suspended membrane was investigated for fixed Si_3N_4 thickness (200 nm) and variable AlN thickness. The phase and group velocity dispersion curves of the first eight Lamb modes travelling along the composite plate were calculated by using the software Disperse [6] and are plotted in figure 1a and b; the abscissa H/λ represents the total waveguide thickness ($H = h_{AlN} + h_{Si3N4}$) to the acoustic wavelength λ ratio.

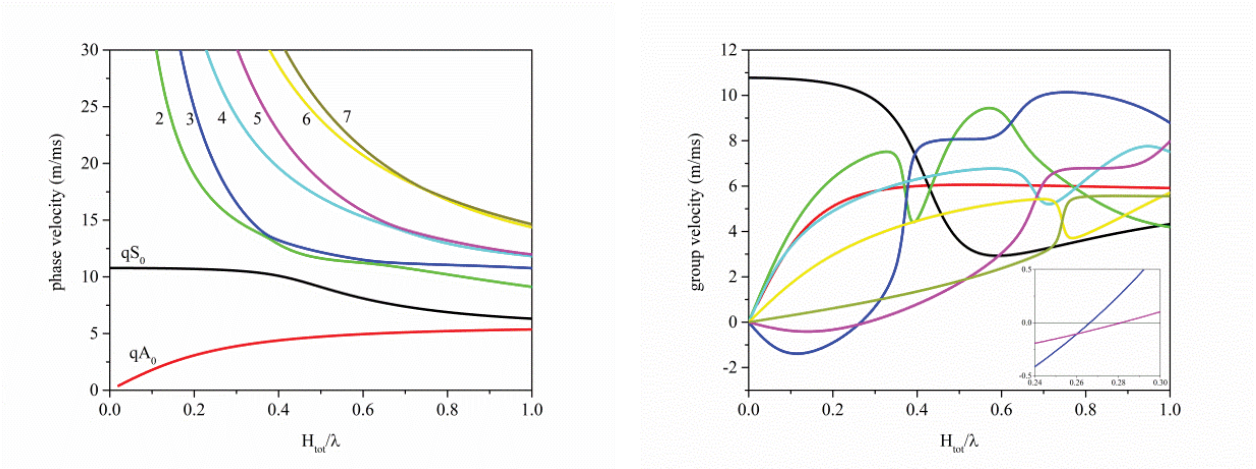

FIGURE 1. a) Phase and b) group velocity dispersion curves of Lamb modes travelling along the AlN(2.8 μm)/Si_3N_4(200 nm) composite plate. Same coloured curves in both figures belong to the same mode.

The distinction between symmetric and antisymmetric Lamb modes in figures 1a and 1b is somewhat artificial for a composite plate since it has no symmetry with respect to its mid-plane. Thus the dispersion curves of figure 1a have been generically distinguished by a number in the order in which the modes appear along the frequency axis after the two fundamental modes labelled qA_0 and qS_0. The Si_3N_4 layer material was considered isotropic and lossless; the AlN layer was considered single crystal and lossless [7], and its stiffened elastic constants were used in the calculations. The geometry of the system is a plate of finite thickness and infinite other dimensions. As it can be seen in figure 1b, some branches, corresponding to the ''backward-wave'' propagation, occur in the negative-slope region where group velocity and phase velocity have opposite signs. For negative group velocities, the direction of propagation of wave energy and that of wave phase are opposite. Figure 1b shows an inset where the ZGV points of the modes 3 and 5 are clearly visible, corresponding to $H_{tot}/\lambda = 0.266$ and 0.283.

Finite element method (FEM) has been carried out by using COMSOL Multiphysics 5.2 to explore the field shape of the ZGV points in the composite waveguide [8-10]. The IDT of the ZGVR was assumed to have N = 5 finger pairs and an aperture $W = 40 \cdot \lambda$; the total length of the composite plate is $20 \cdot \lambda$, thus the presence of the silicon frame was not accounted in the FEM. AlN was assumed to have an elastic loss $\tan\delta = 0.002$. Figure 2 shows the schematic of the ZGVR.

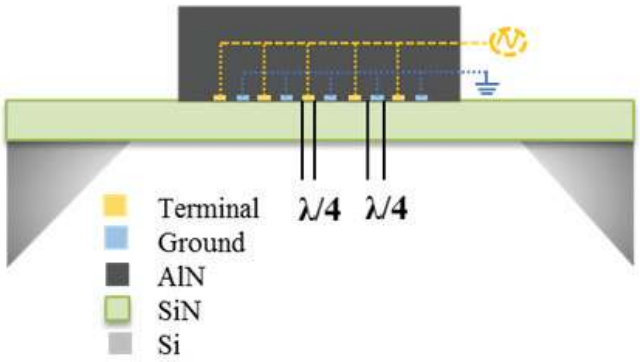

FIGURE 2. The schematic of the ZGVR.

Traction free boundary conditions were selected for the top and bottom sides of the composite plate, while perfectly matched layer (PML) boundary condition were selected for the right and left end sides of the waveguide. The total absolute displacement of the two ZGV3 and ZGV5 modes travelling along the AlN(2.8 μm)/SiN(200 nm) suspended membrane are shown in figures 3a-b: the color density bar is representative of the relative particle displacement. As it can be seen in figures 3a-b, the acoustic field of the ZGV3 and ZGV5 modes is localized only under the IDT: the horizontal black line represents the interface between the Si_3N_4 and the AlN layers; the two vertical black lines, on left and right sides of the device, represent the PML boundary conditions. The PML was used to model a domain with open boundaries through which the wave pass without undergoing any reflection.

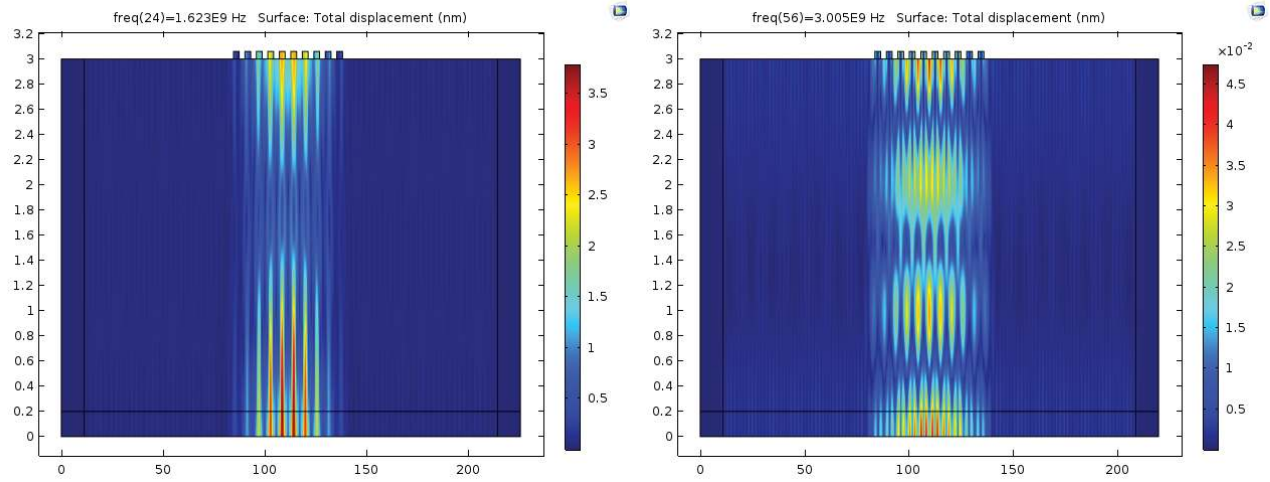

(a) (b)

FIGURE 3. The field profile of a) ZGV3 mode for $H_{tot}/\lambda = 0.266$, b) ZGV5 mode for $H_{tot}/\lambda = 0.283$; $H_{tot} = 3$ μm.

The 2D eigen-frequency study of the ZGVR3 was performed by considering the presence and the mass loading of the Cr(10 nm)/Au(60 nm) IDT, and by applying an alternate drive voltage to the electrodes. The electric potential of the IDT fingers are alternately set as +1 V (terminal) and 0 V (ground), whereas all other electric boundary conditions are set to zero charge/symmetry. The calculations were performed without and with the PML on left and right sides of the device. The PML simulations made "without PML" imply that the wave reflection at the boundaries is accounted. The ZGVRs absolute admittance Y vs frequency curves of the modes that propagate in the AlN/Si_3N_4 membrane, with and without a PML, are shown in figure 4. As it can be seen, a strong resonance corresponds to the qS_1 mode for the frequency value corresponding to the ZGV3.

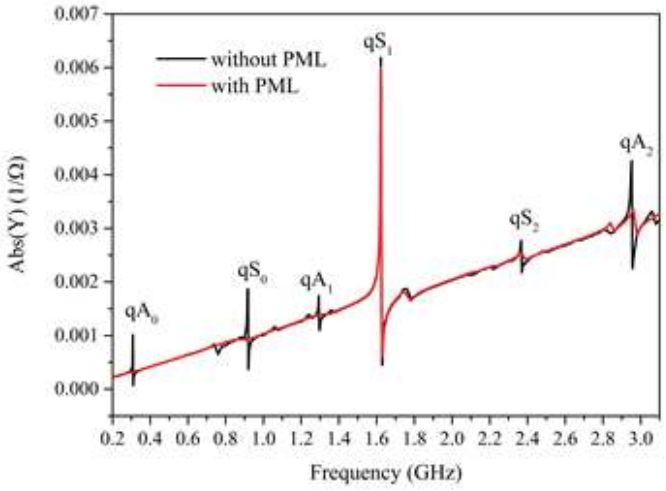

FIGURE 4. The absolute admittance Y vs frequency curves of the AlN/Si_3N_4 plate ($H_{tot}/\lambda = 0.266$, $H_{tot} = 3\mu m$), with and without a PML.

The two curves of figure 4 confirm that the ZGV resonant peak are unaffected by the presence of the PML as opposed to the other propagating modes. From these curves the resonator $Q = f_r/BW$ and electroacoustic coupling efficiency $K^2 = \pi^2 \cdot (f_p - f_s)/4 \cdot f_p$ were calculated [11], where f_r is the conductance peak frequency, BW is the full bandwidth at half maximum of the conductance peak, f_p and f_s are the parallel and series resonance frequencies extracted from the susceptance curve: Q = 510 and 357 for ZGV3 and ZGV5, and K^2 =0.52% and 0.63% for the 3 and 5 mode. The theoretically expected ZGV3 and ZGV5 resonant frequencies are 1.62 and 2.96 GHz fot H_{tot} = 3 μm.

DEVICE FABRICATION PROCESS AND TEST

Conventional electroacoustic devices implemented onto thin suspended piezoelectric membranes are fabricated onto double side polished silicon (100) wafers covered by a thin SiO_2 or Si_3N_4 layer on both sides. The technological process flow includes several steps, such as the growth of the piezoelectric layer onto the upper side of the substrate, the IDT photolithographic patterning, then the definition of the etch window on the lower surface of the substrate. The final step consists in the back side Si bulk dry or wet etching up to the SiO_2 or Si_3N_4 stop etchant to provide the release of the suspended membrane [12]. The present ZGVR was fabricated directly onto commercially available thin Si_3N_4 suspended membrane (200 nm thick, with area of 1.5 mm x 1.5 mm) carried by a square Silicon frame, 200 μm thick (area 5 mm x 5mm). The IDT pattern was defined by electron beam lithography (EBL) and lift off process of a Cr(10 nm)/Au(60 nm) layer. Figure 5a shows a photo of the Cr/Au IDT patterned onto the central part of the thin Si_3N_4 membrane. Finally the AlN film was deposited by sputtering technique, at room temperature, onto the Si_3N_4 membrane by using a shadow mask with an opening area of 1 mm^2 to create an "island-like" structure of AlN, centered onto the IDT, as shown in figure 2. The AlN film was uniform, crack-free, and highly adhesive to the membrane.The crystal structure and the preferred orientation of the AlN films were investigated by x-ray diffraction. The ϑ–2ϑ diffraction pattern shows polycrystalline hexagonal structure. The strongest peak at approximately 2ϑ = 36° corresponds to the (0002) reflection and it is dominant, indicating a strong alignment of the AlN grains along the c-axis perpendicular to the membrane surface. The degree of the film orientation along the c-axis was measured by rocking curves of the (0002) peak. The full widths at half maximum (FWHM) was about 2°. To simplify the technological process, the Cr/Au IDT periodicity was chosen to be equal to 10 μm: as a consequence, a different plate thickness (H_{tot} = 2.7 μm) and ZGV resonant frequency (1.78 GHz) are the new ZGV3-based resonator design parameters.

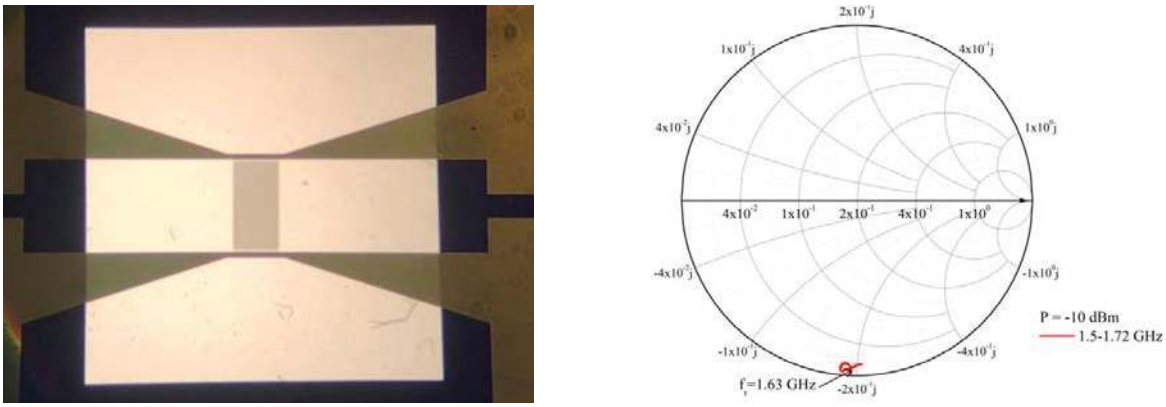

(a) (b)

FIGURE 5. a) A photo of the Cr/Au IDT patterned onto the thin Si_3N_4 membrane (λ = 10 μm); b) The Smith chart of the ZGVR.

The scattering parameter S_{22} of the resonator was measured with a vectorial network analyser (Agilent N5230A) connected to a microprobe station (Cascade-SUMMIT 9101). Figure 5b shows the Smith chart of the S_{22} scattering parameter of the ZGVR. The resonant frequency is 1.63 GHz, corresponding to a phase velocity of 16300 m/s. The discrepancy between the theoretical (about 1.78 GHz) and the experimental resonant frequencies may be attributed to several factors, such as the polycrystalline nature of the AlN film (while single-crystal AlN was assumed in the theoretical calculations), the non-uniform thickness of the AlN film growth onto the IDT's metal electrodes, and the accuracy of the AlN layer thickness control. As the ZGV point belongs to a highly dispersive branch of the mode dispersion curve, the layer thickness is critical to the resonant frequency control: a small thickness change corresponds to a large resonant frequency shift. A better accuracy in the film thickness control, the choice of IDT with lower mass loading effect, and the presence of few grounded guarding strips on each side of the IDT (as in reference 1) will result in improved ZGVR performances.

CONCLUSIONS

The technological feasibility of the ZGVR on commercial Si_3N_4 suspended membrane is demonstrated and preliminary results concerning the first symmetric mode ZGV point are shown. Works are in progress to fabricate ZGVRs onto composite membranes, including a piezoelectric and a non-piezoelectric layer, in order to test higher order ZGV points.

ACKNOWLEDGMENTS

This work has received funding from the European Union' Horizon 2020 Research and Innovation Programme under the Marie Sklodowska-Curie Grant Agreement No. 642688. The authors want to thank Dr. Jorge Pedros and Mr. Rajveer Fandan from Universidad Politécnica de Madrid for the device test and XRD measurements.

.

REFERENCES

1. Hashimoto, Ken-Ya, *Surface Acoustic Wave Devices in Telecommunications, Modelling and Simulation* (Springer-Verlag, Berlin Heidelberg, 2000), pp. 184-188.
2. Bjurstrom J, Katardjiev I and Yantchev V, Appl. Phys. Lett. **86**, 154103 (2005).
3. C.-M. Lin, Y.-J. Lai, J.-C. Hsu, Y.-Y. Chen, D. G. Senesky, and A. P. Pisano, Appl. Phys. Lett. **99**, 143501 (2011).

4. V. Yantchev, L. Arapan, I. Ivanov, I. Uzunov, I. Katardjiev, V. Plessky, in *Proceedings of the IEEE International Ultrasonics Symposium*, 2012, pp. 307-310.
5. V. Yantchev, L. Arapan, I. Katardjiev, and V. Plessky, Appl. Phys. Lett. **99**, 033505 (2011).
6. Lowe M and Pavlakovic B, Disperse Software, v. 2.0.20a-compiled 10 October 2013, Copyright 1996–2013 (licensed by Imperial College Consultant, serial number F21122C).
7. K. Tsubouchi and N. Mikoshiba, IEEE Trans. Sonics Ultrason. **SU-32**, 634 (1985).
8. C Caliendo, M Hamidullah, "Pressure sensing with Zero Group Velocity Lamb modes in self-supported a-SiC/c-ZnO membranes", submitted to Journal of Physics D: Applied Physics.
9. C. Caliendo, M. Hamidullah, in *Proceedings of the 4th International Electronic Conference on Sensors and Applications*, 2018, Edited by MDPI, Basel, **2**, 133.
10. C Caliendo, M Hamidullah, Journal of Physics D: Applied Physics, **50**, 474002 (2017).
11. W. Soluch, IEEE Trans. Ultrason., Ferroelectr., Freq. Control, **47**, 1615-1518 (2000).
12. S. Mendoza-Acevedo, M. A. Reyes-Barranca, E. N. Vázquez-Acosta, J. A. Moreno-Cadenas and J. L. González-Vidal , "Release Optimization of Suspended Membranes in MEMS", in *Micromachining Techniques for Fabrication of Micro and Nano Structures*, edited by Mojtaba Kahrizi, (InTech, Rijeca, Croatia, 2012), pp. 183–204.